

Itinerant ferromagnetism in half-metallic CoS₂

S. K. Kwon, S. J. Youn,* and B. I. Min

Department of Physics, Pohang University of Science and Technology, 790-784 Pohang, Korea

(Received 14 January 2000)

We have investigated electronic and magnetic properties of the pyrite-type CoS₂ using the linearized muffin-tin orbital band method. We have obtained the ferromagnetic ground state with nearly half-metallic nature. The half-metallic stability is studied by using the fixed spin moment method. The non-negligible orbital magnetic moment of Co 3*d* electrons is obtained as $\mu_L = 0.06\mu_B$ in the local spin-density approximation (LSDA). The calculated ratio of the orbital to spin angular momenta $L_z/S_z = 0.15$ is consistent with experiment. The effect of the Coulomb correlation between Co 3*d* electrons is also explored with the LSDA + *U* method. The Coulomb correlation at Co sites is not so large, $U \lesssim 1$ eV, and so CoS₂ is possibly categorized as an itinerant ferromagnet. It is found that the observed electronic and magnetic behaviors of CoS₂ can be described better by the LSDA than by the LSDA + *U*.

I. INTRODUCTION

Transition-metal disulfides of MS_2 ($M = \text{Fe, Co, Ni, etc.}$) with the pyrite structure show a variety of physical properties. Electronic and magnetic properties of the MS_2 has been qualitatively explained by the successive filling of the e_g band of metal ions. In the NaCl-type structure of pyrite MS_2 , divalent metal ions of M^{2+} are located at the center of octahedron formed by S_2^{2-} dimers. Hence, the M -3*d* bands are split into t_{2g} and e_g subbands due to large crystal field. The M -3*d* electron configuration varies from $t_{2g}^6 e_g^0$, $t_{2g}^6 e_g^1$, to $t_{2g}^6 e_g^2$ for FeS₂, CoS₂, and NiS₂. All of them are in the low-spin states, $S = 0$, $S = 1/2$, and $S = 1$ for FeS₂, CoS₂, and NiS₂, respectively. With fully occupied t_{2g}^6 and completely empty e_g^0 bands, FeS₂ is a semiconductor with an energy gap of $E_g \approx 0.8$ eV.¹ CoS₂ is a ferromagnetic metal with $T_C \approx 120$ K.^{2,3} NiS₂ is an antiferromagnetic insulator ($T_N \approx 40$ K) with a half-filled e_g^2 band due to the large on-site Coulomb correlation.^{4,5}

Despite extensive studies on these systems, the electronic and magnetic properties of CoS₂ are not fully understood yet. The issues for CoS₂ to be resolved are (i) whether it is a strongly correlated electron system, (ii) whether it is classified as an itinerant electron ferromagnet, and (iii) whether it is a half-metal or not. It is considered that Co 3*d* states in CoS₂ are just at the boundary of the localized and delocalized regime.⁴ Magnetic measurement using polarized neutron diffraction indicates that most of the magnetic moment is localized at Co sites.⁶ The analysis of photoemission spectroscopy (PES) data for CoS₂ in terms of the cluster model calculations yields a large Coulomb correlation parameter, $U = 3.0\text{--}4.2$ eV.^{5,7} According to the magnetic circular dichroism (MCD) measurements, a non-negligible orbital magnetic moment is observed for Co 3*d* electrons, $L_z/S_z = 0.18$ (Ref. 7) and 0.14.⁸ Such an unquenched orbital moment is exceptional, considering the low-spin state of Co 3*d* electrons in CoS₂ with a large crystal-field splitting of $10D_q \approx 2.5$ eV. On the other hand, transport properties of

CoS₂ are known to be well described by the itinerant electron model.^{9,10} Further, the dynamical susceptibility measured by the inelastic magnetic neutron scattering¹¹ and optical properties¹² are analyzed based on the itinerant band model.

Using the linearized atomic orbitals band method, Zhao *et al.*¹³ have found that CoS₂ is close to half-metallic in the sense that the occupation number of the minority-spin e_g band is very small compared to that of the majority-spin e_g band. More recently, Hobbs and Hafner¹⁴ have studied the ground-state cohesive properties of CoS₂ and obtained similar results using the projected augmented wave band method. In fact, recent experimental reflectivity data have been consistently interpreted under the assumption of half-metallic CoS₂.¹² In contrast, the linearized muffin-tin orbital (LMTO) band calculation by Yamada *et al.*¹⁵ gives rise to the normal-metallic ferromagnetic ground state with a partially filled minority-spin e_g band.

To clarify the above-mentioned issues and to resolve the differences between existing band calculations, we have re-examined electronic and magnetic properties of CoS₂ using the LMTO band method. Both the local spin-density approximation (LSDA) and the LSDA + *U* approximation¹⁶ are employed to explore the effect of the Coulomb correlation interaction between Co 3*d* electrons. The von Barth–Hedin form of the exchange-correlation potential is utilized. Further, the fixed spin moment method is used to check the stability of the half-metallic state. We have also estimated the orbital contribution to the total magnetic moment in CoS₂, using the fully relativistic calculations in which the spin-orbit coupling is simultaneously included in the self-consistent variational loop.¹⁷

II. COMPUTATIONAL DETAILS

Formally, the LSDA + *U* Hamiltonian is constructed as follows:

$$\begin{aligned}
\mathcal{H}_{\text{LSDA}+U} &= \mathcal{H}_{\text{LSDA}} - \mathcal{H}_{\text{dc}} \\
&+ \frac{1}{2} \sum_{\{m\}, \sigma} V(mm'; m''m''') n_{mm''}^{\sigma} n_{m'm'''}^{-\sigma} \\
&+ \frac{1}{2} \sum_{\{m\}, \sigma} \{V(mm'; m''m''') \\
&- V(mm'; m''m''')\} n_{mm''}^{\sigma} n_{m'm'''}^{\sigma}, \quad (1)
\end{aligned}$$

where $n_{mm''}^{\sigma}$ is the d occupation number matrix of spin σ and $\mathcal{H}_{\text{dc}} = -\frac{1}{2}UN(N-1) + \frac{1}{2}J\sum_{\sigma}N^{\sigma}(N^{\sigma}-1)$ with $N^{\sigma} = \sum_m n_{mm''}^{\sigma}$ and $N = \sum_{\sigma} N^{\sigma}$. The screened Coulomb interaction $V(mm'; m''m''')$ is related to the Slater integral F^k by

$$V(mm'; m''m''') = \sum_{k=0}^{2l} c^k(lm, lm'') c^k(lm''', lm') F^k, \quad (2)$$

where $c^k(lm, lm')$ is a Gaunt coefficient. Two main parameters in the LSDA+ U method are the Coulomb U and the exchange J interactions. The relations of these parameters to the Slater integrals are given by $U = F^0$ and $J = (F^2 + F^4)/14$. The ratio of F^4/F^2 is known to be constant around 0.625 for most 3d transition-metal atoms.¹⁸ We have used parameter values of $U = 0.0$ – 4.0 eV with a fixed $J = 0.89$ V.

The crystal structure of pyrite CoS_2 is cubic with the lattice constant of $a = 5.528$ Å, and the space group is $T_h^6(Pa\bar{3})$. There are 24 symmetry operations. The four Co atoms are located at positions ($4a$): (0,0,0), (1/2,0,1/2), (0,1/2,1/2), and (1/2,1/2,0). The eight S atoms are at positions ($8c$): (u, u, u), ($u + 1/2, u, \bar{u} + 1/2$), ($u, \bar{u} + 1/2, u + 1/2$), and ($\bar{u} + 1/2, u + 1/2, u$), where we have used the position parameter of $u = \pm 0.389$. To improve the packing ratio, 24 empty spheres are introduced at positions ($24d$). For the Brillouin zone (BZ) integration, the tetrahedron method is adopted with 80 k points sampling in the irreducible BZ wedge. The LMTO basis functions are included up to $l=2$ for Co, and $l=1$ for S and empty spheres.

III. ELECTRONIC STRUCTURES AND MAGNETIC PROPERTIES

In Fig. 1, we show the LSDA density of states obtained at the experimental lattice constant. Because of the strong covalent bonding nature of S-S dimers, each S band can be identified with molecular orbitals. The two peaks in the highest binding energy side are the bonding S $3s\sigma$ and the antibonding S $3s\sigma^*$ bands, respectively.¹⁹ The broad band of about 6-eV width between -4 and -10 eV consists mainly of S $3p$, which is a mixture of $3p\sigma$, $3p\pi$, and $3p\pi^*$ bands. The antibonding S $3p\sigma^*$ intradimer band is located at about 2.5 eV above the Fermi energy E_F . The spin split bands of Co t_{2g} are located between -1 and -3 eV below E_F , while the Co e_g band is near E_F . It is seen that Co 3d bands are formed in the energy range between S $3p$ and S $3p\sigma^*$ bands. The t_{2g} band is nearly dispersionless with very narrow band width, whereas the e_g band near E_F is dispersive with a relatively large band width of about 2.5 eV due to strong hybridization with the S $3p\sigma^*$ band. The nearly half-

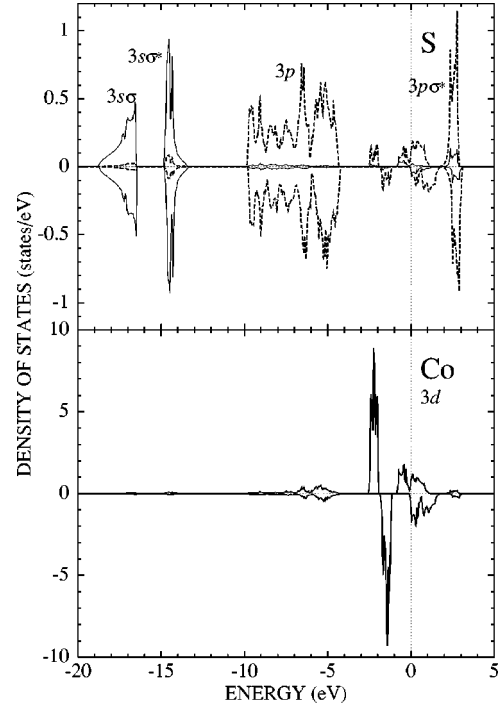


FIG. 1. The LSDA DOS of pyrite CoS_2 at each atomic site. The two peaks at the highest binding energy side (upper panel) are bonding and antibonding S $3s$ bands, respectively. The antibonding S $3p\sigma^*$ band is located at about 2.5 eV above E_F . The spin split Co $3d$ bands, t_{2g} and e_g , are formed between S $3p$ and S $3p\sigma^*$ bands (lower panel). The e_g band near E_F manifests the nearly half-metallic nature of CoS_2 .

metallic nature and the exchange splitting $\Delta_X \sim 1.0$ eV are prominent for the e_g band.

The present results are slightly different from those of existing calculations.^{13,15} In Ref. 13, the S $3p\sigma^*$ band is at ~ 1.5 eV above E_F which is lower than the present result by about 1.0 eV, whereas, in Ref. 15, the states of the S $3p\sigma^*$ band is smeared out by too strong hybridization with Co e_g bands. The bremsstrahlung isochromat spectrum (BIS) shows clear double-peak structure at about 1.0 and 2.5 eV above E_F ,²⁰ which is more consistent with the present result. That is, the 1.0-eV peak corresponds to the minority-spin e_g band and the 2.5-eV peak to S $3p\sigma^*$ band. The occupation of the minority-spin e_g band is only 0.04 electrons/Co, reflecting that CoS_2 is almost half-metallic. This feature is in agreement with that obtained by Zhao *et al.*¹³ In the analysis of the reflectivity data in terms of the half-metallic CoS_2 ,¹² the minority-spin e_g band is assigned at about 1.5 eV above E_F . This is close to but a bit higher than the present LSDA result.

Figure 2 is the LSDA total energy as a function of the lattice constant. The ferromagnetic ground state is lower in energy than the paramagnetic state even far below the experimental lattice constant of $a = 5.528$ Å, represented by the arrow. The minimum of the total energy is located near the experimental lattice constant for both the paramagnetic and the ferromagnetic states, and thus the LSDA seems to describe well the cohesive bonding properties of CoS_2 .¹⁴ The ferromagnetic ground state is lower in energy by about 10 mRy than the paramagnetic state at the experimental lattice

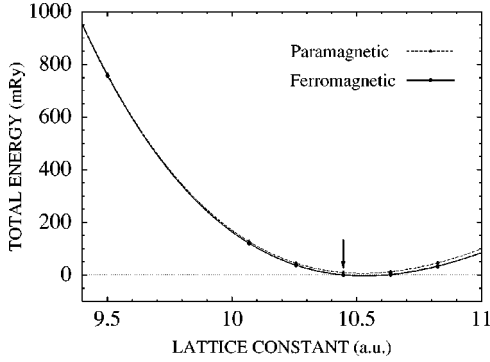


FIG. 2. The LSDA total energy as a function of lattice constant. The arrow indicates the experimental lattice constant. The ferromagnetic ground state is lower in energy than the paramagnetic state far below the experimental lattice constant.

constant. The energy difference between the ferromagnetic and the paramagnetic states decreases with decreasing the lattice constant. This is contrary to the result of Yamada *et al.*¹⁵ in which the paramagnetic is stable near the experimental lattice constant and the ferromagnetic state becomes stable only for $a > 5.57 \text{ \AA}$. As they pointed out, it seems to be ascribed to the small number of k points they used. On the basis of the total-energy curve shown in Fig. 2, the observed metamagnetic transition behavior under the high magnetic field, the high external pressure, and the chemical pressure by substituting Se in place of S can be qualitatively understood.^{10,21}

By using the fixed spin moment method within the LSDA, the total energy is evaluated with varying the magnetic moment in CoS₂ (Fig. 3). For all the fixed spin moments, $0.00\mu_B < M \leq 4.00\mu_B$, the ferromagnetic state is stable as compared to the paramagnetic state. The spin direction of S atoms is always parallel to that of Co. The ground state is found for $M = 3.66\mu_B$ (denoted by the arrow), which is a normal ferromagnetic metal and lower in energy by about 10 mRy than the paramagnetic state. It is noticeable that the half-metallic state with exact integer magnetic moment of $M = 4.00\mu_B$ is very close in energy to the normal-metallic ground state. The total-energy difference between the normal-metallic ground state and the half-metallic state is less than 0.1 mRy because of quite small electron occupation of the minority-spin e_g band in the ground state. Thus, it is expected that, with only a small number of hole doping, the half-metallic state can be realized in CoS₂.¹³

In general, a polycrystalline half-metallic system is expected to show large magnetoresistance (MR) behavior. It arises from the activated electron tunneling mechanism at the grain boundary with the applied external magnetic field.²² To our knowledge, there has been no report available on the MR measurement for CoS₂. Therefore, the MR measurement on polycrystalline CoS₂ and Fe_xCo_{1-x}S₂ is desirable to exploit the correlation between the half-metallic nature and the MR.

We have applied the LSDA and the LSDA+ U methods to explore the Coulomb correlation effect on the magnetic properties. The observed magnetic moments per Co atom are in the range of $0.84\text{--}0.91\mu_B$.^{3,12} The orbital magnetic moment in CoS₂ is obtained by including the spin-orbit coupling in the total Hamiltonian. In the LSDA+ U calculations, we have used fixed J ($=0.89 \text{ eV}$), which is insensitive to

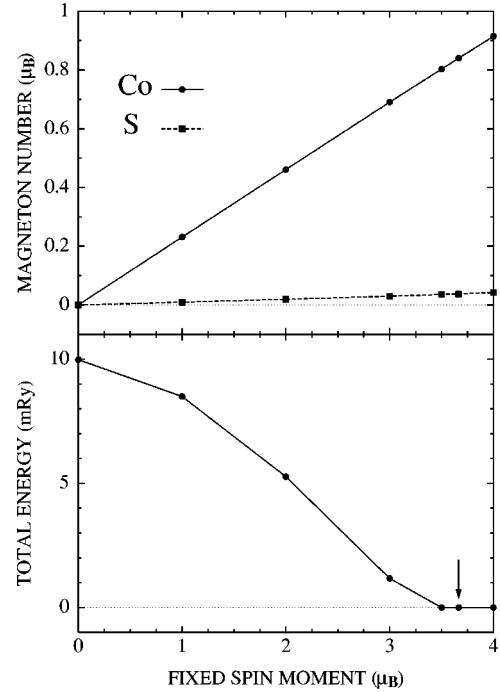


FIG. 3. The behavior of the spin magnetic moment at each site (upper panel) and the total energy (lower panel) with varying the total spin magnetic moment M (μ_B) in the unit cell. The arrow denotes the normal-metallic ferromagnetic ground state with $M = 3.66\mu_B$. The half-metallic state with integer $M = 4.00\mu_B$ is very close in energy to the normal-metallic ground state.

the the local environment. In the LSDA, we have obtained the spin and orbital magnetic moments per Co atom, $\mu_S = 0.80\mu_B$ and $\mu_L = 0.06\mu_B$, respectively (Table I). This produces the ratio of $L_z/S_z = 0.15$, which is close to the MCD measurement of $L_z/S_z = 0.18$ (Ref. 7) and 0.14 .⁸ The total magnetic moment per Co atom $\mu_{tot} = 0.86\mu_B$ in the LSDA is also in agreement with the experiment.

Both the spin and orbital magnetic moments increase with

TABLE I. Calculated spin and orbital magnetic moments μ_S and μ_L (μ_B) of CoS₂ for various Coulomb correlation U (eV) (J is fixed as 0.89 eV). All the results are from the relativistic calculations. M_{fu} (μ_B) is the total magnetic moment per formula unit. The total magnetic moment per Co atom $\mu_{tot} = 0.86\mu_B$ and the ratio of $L_z/S_z = 0.15$ in the LSDA is consistent with experimental data.

U	M_{fu}		Co	S
0.0	0.90	μ_S	0.76	0.04
		μ_L	0.06	0.00
1.0	1.06	μ_S	0.88	0.04
		μ_L	0.10	0.00
2.0	1.13	μ_S	0.93	0.03
		μ_L	0.14	0.00
3.0	1.21	μ_S	1.01	0.00
		μ_L	0.20	0.00
4.0	1.25	μ_S	1.07	-0.03
		μ_L	0.25	0.00
LSDA	0.93	μ_S	0.80	0.04
		μ_L	0.06	0.00

increasing the Coulomb correlation parameter U . For $U \geq 3.0$ eV, the minority-spin e_g band moves to higher-energy states and CoS_2 becomes completely half-metallic. For $U = 4.0$ eV, the minority-spin e_g band is formed at about 2.0 eV above E_F . However, the discrepancy of the total magnetic moment between the experiment and the theory becomes significant for $U \geq 2.0$ eV. Moreover, the ratio of $L_z/S_z = 0.31$ for $U = 2.0$ eV is too large compared to the experimental values.^{7,8} This finding suggests that the size of the on-site Coulomb correlation in CoS_2 is to be rather small $U \leq 1$ eV, and the LSDA gives a better description of Co $3d$ states in CoS_2 . Note that the local-density approximation results for FeS_2 show an excellent agreement with PES and BIS data.^{23,24} In addition, the weak satellite feature in the PES of CoS_2 (Ref. 5) seems to be consistent with the present results of rather small Coulomb correlation U .

Finally, let us remark on the electronic structure of CoS_2 in its paramagnetic phase ($T > T_C$). As mentioned in the Introduction, it is an unresolved issue. The question is whether the exchange splitting in Co $3d$ bands persists above T_C or not. The present study reveals that the width of the Co e_g band is larger than both the Coulomb correlation interaction U and the exchange splitting Δ_X . It thus suggests that the Co $3d$ electrons near E_F will behave as itinerant to manifest Stoner-type magnetic phenomena at the finite temperature. Indeed, there are such evidences from several experiments. Resonance PES data for Co $3d$ bands taken at temperatures across the magnetic transition indicate a slight but noticeable spectral change between the paramagnetic and the ferromagnetic phases, reflecting the long-range spin-exchange effect.²⁵ Optical spectra above T_C are described well using

the itinerant Stoner model.¹² Also, inelastic magnetic neutron-scattering data above T_C exhibit the Stoner excitations stemming from the itinerant electrons.¹¹ On the other hand, based on the PES studies, it is claimed that the electronic structure in the paramagnetic phase should be described by the local band picture.^{5,20} Hence, further studies are necessary to ascertain this point.

IV. CONCLUSION

We have investigated the electronic and magnetic properties of the pyrite-type CoS_2 using the LMTO band method. We have found the following results: (i) CoS_2 does not belong to the strongly correlated electron system, because the effect of the Coulomb correlation at Co sites is rather small, $U \leq 1$ eV, (ii) CoS_2 can be categorized as an itinerant electron ferromagnet, since the band width of Co e_g state is larger than U and the exchange splitting Δ_X , (iii) CoS_2 is nearly half-metallic in that the half-metallic state is very close in energy to the normal-metallic ground state. A non-negligible orbital magnetic moment of Co $3d$ electrons is obtained as $\mu_L = 0.06\mu_B$ in the LSDA, which is consistent with experiment. Accordingly, the electronic and magnetic properties of CoS_2 are described better with the LSDA than with the LSDA+ U .

ACKNOWLEDGMENTS

The authors would like to thank Jin Ho Park for helpful discussions. This work was supported by the KOSEF (1999-2-114-002-5) and in part by the Korean MOST-FORT fund.

*Present address: Department of Physics, Northwestern University, Evanston, Illinois 60208-3112.

¹E.K. Li, K.H. Johnson, D.E. Eastman, and J.L. Freeouf, Phys. Rev. Lett. **32**, 470 (1974).

²A.F. Andresen, S. Furuseth, and A. Kjekshus, Acta Chem. Scand. **21**, 833 (1967).

³K. Adachi, K. Sato, and M. Takeda, J. Phys. Soc. Jpn. **26**, 631 (1969).

⁴J.A. Wilson, Adv. Phys. **21**, 143 (1972).

⁵A. Fujimori, K. Mamiya, T. Mizokawa, T. Miyadai, T. Sekiguchi, H. Takahashi, N. Mori, and S. Suga, Phys. Rev. B **54**, 16 329 (1996).

⁶A. Ohsawa, Y. Yamaguchi, H. Watanabe, and H. Itoh, J. Phys. Soc. Jpn. **40**, 986 (1976).

⁷T. Muro, T. Shishidou, F. Oda, T. Fukawa, H. Yamada, A. Kimura, S. Imada, S. Suga, S. Y. Park, T. Miyahara, and K. Sato, Phys. Rev. B **53**, 7055 (1996).

⁸H. Miyauchi, T. Koide, T. Shidara, N. Nakajima, H. Kawabe, K. Yamaguchi, A. Fujimori, H. Fukutani, K. Iio, and T. Miyadai, J. Electron Spectrosc. Relat. Phenom. **78**, 255 (1996).

⁹H.S. Jarrett, W. H. Cloud, R. J. Bouchard, S. R. Butler, C. G. Frederich, and J. L. Gillson, Phys. Rev. Lett. **21**, 617 (1968).

¹⁰K. Adachi, M. Matsui, and M. Kawai, J. Phys. Soc. Jpn. **46**, 1474 (1979).

¹¹H. Hiraka, Y. Endoh, and K. Yamada, J. Phys. Soc. Jpn. **66**, 818 (1997).

¹²R. Yamamoto, A. Machida, Y. Moritomo, and A. Nakamura, Phys. Rev. B **59**, R7793 (1999).

¹³G.L. Zhao, J. Callaway, and M. Hayashibara, Phys. Rev. B **48**, 15 781 (1993).

¹⁴D. Hobbs and J. Hafner, J. Phys.: Condens. Matter **11**, 8197 (1999).

¹⁵H. Yamada, K. Terao, and M. Aoki, J. Magn. Magn. Mater. **177-181**, 607 (1998).

¹⁶V.I. Anisimov, J. Zaanen, and O.K. Andersen, Phys. Rev. B **44**, 943 (1991); A.I. Liechtenstein, V.I. Anisimov, and J. Zaanen, *ibid.* **52**, R5467 (1995).

¹⁷B.I. Min and Y.-R. Jang, J. Phys.: Condens. Matter **3**, 5131 (1991).

¹⁸F.M.F. de Groot, J.C. Fuggle, B.T. Thole, and G.A. Sawatzky, Phys. Rev. B **42**, 5459 (1990).

¹⁹D.W. Bullet, J. Phys. C **15**, 6163 (1982).

²⁰K. Mamiya, T. Mizokawa, A. Fujimori, H. Takahashi, N. Mori, T. Miyadai, S. Suga, N. Chandrasekharan, S. R. Krishnakumar, and D. D. Sarma, Physica B **237-238**, 390 (1997).

²¹T. Goto, Y. Shindo, H. Takahashi, and S. Ogawa, Phys. Rev. B **56**, 14 019 (1997).

²²H.Y. Hwang, S.-W. Cheong, N.P. Ong, and B. Batlogg, Phys. Rev. Lett. **77**, 2041 (1996).

²³W. Folkerts, G. A. Sawatzky, C. Haas, R. A. de Groot, and F. U. Hillebrecht, J. Phys. C **20**, 4135 (1987).

²⁴M. Imada, A. Fujimori, and Y. Tokura, Rev. Mod. Phys. **70**, 1039 (1998).

²⁵T. Muro, A. Kimura, T. Iwasaki, S. Ueda, S. Imada, T. Matsushita, A. Sekiyama, T. Susaki, K. Mamiya, T. Harada, T. Kanomata, and S. Suga, J. Electron Spectrosc. Relat. Phenom. **88**, 91 (1998).